

Topological phase preparation in a pair of atomic Bose-Einstein condensates

J. Ruostekoski

Abteilung für Quantenphysik, Universität Ulm, D-89069 Ulm, Germany

(May 28, 2017)

We propose a method of generating skyrmion vortices in a pair of Bose-Einstein condensates occupying two internal states of the same atom. We show that a variety of different periodic arrays of vortices may be prepared with an appropriate superposition of orthogonal standing electromagnetic waves inducing a coherent coupling between the two condensates.

03.75.Fi,05.30.Jp

Since the first observations of Bose-Einstein condensation in dilute atomic gases [1–3] one important goal has been to develop a technology to investigate vortices in atomic Bose-Einstein condensates (BECs). The quantized vortices in atomic BECs are analogous to the quantized circulation in superfluid liquid helium [4]. In this paper we propose a method of generating different periodic patterns of skyrmion vortices and solitary waves in a pair of atomic BECs. The two condensates are coupled by electromagnetic (em) transitions. The em fields form a standing wave configuration with topological singularities at zero-field points. The em field amplitude couples to the relative phase between the two BECs through the atomic transitions. As a result the Rabi oscillations of atoms between the two internal states generate an array of topological phases in the two condensate system.

A BEC is expected to exhibit vorticity in a rotating harmonic trap if the trap is anisotropic in the plane of rotation [5–9]. It has also been proposed that stirring a BEC in a nonrotating configuration by a laser beam [10–12] or by an optically-induced potential [13] may generate vortices. Topological defects may also emerge as a result of a rapid condensation [14] or in self-interference measurements [15]. Recently, it has been suggested that vorticity could be imprinted by imaging a BEC through an absorption plate [16,17]. Phase-imprinted dark solitons have been observed in an atomic BEC [17,18].

While the previously explained schemes typically involve a BEC in a single internal atomic state several papers [19–21] have also considered the possibility of transferring an atomic population from a nonrotating ground state to a vortex state by means of a Laguerre-Gaussian laser beam consisting of photons with a nonvanishing orbital angular momentum. In a very recent work Williams and Holland [22] have proposed a scheme where two internal states are coupled and the trapping potentials of these states are mechanically rotated. This technique has been experimentally realized to demonstrate the formation of a vortex in a two-component BEC [23].

In this paper we propose a method of generating vortices which is related to the previously described schemes [19–22] involving internal atomic transitions. We consider two internal states of the same atom which are coupled by em fields via one or multiphoton transitions. The em fields consist of two or more orthogonal standing waves. With an appropriate wave configuration we obtain a spatially-dependent transition strength with angular momentum singularities at zero-field points. As a result of the spatially-dependent driving the internal and external dynamics of the atoms are coupled: Around every zero-field point we generate for the two-component BEC a topological phase with an integer multiple of 2π phase winding. The proposed scheme has several advantages: It may be possible to prepare high-quality vortices with little noise. The location of an individual vortex may be accurately controlled by shifting the zero-field point. We may also engineer a large selection of different periodic arrays of vortices in the two-condensate system, where the periodicity is determined by the driving em fields. Moreover, with moving standing em waves we can move the positions of the zero-field points, and therefore, also the vortex array in a controlled way.

The dynamics of the two-component BEC occupying internal levels $|1\rangle$ and $|2\rangle$ follows from the coupled Gross-Pitaevskii equation (GPE)

$$i\hbar\psi_1 = (H_1^0 + \kappa_{11}|\psi_1|^2 + \kappa_{12}|\psi_2|^2)\psi_1 + \hbar\Omega^*\psi_2, \quad (1a)$$

$$i\hbar\psi_2 = (H_2^0 + \delta + \kappa_{22}|\psi_2|^2 + \kappa_{12}|\psi_1|^2)\psi_2 + \hbar\Omega\psi_1. \quad (1b)$$

Here the kinetic energy and the trapping potential are introduced in H_i^0 :

$$H_i^0 \equiv -\frac{\hbar^2}{2m}\nabla^2 + \frac{1}{2}m\omega_i^2(x^2 + \alpha_i^2 y^2 + \beta_i^2 z^2). \quad (2)$$

We have also defined the coefficients of the nonlinearities as $\kappa_{ij} \equiv 4\pi\hbar^2 a_{ij}N/m$. Here a_{ii} denotes the intraspecies scattering length in internal level $|i\rangle$ and a_{12} stands for the interspecies scattering length. The Rabi frequency, $\Omega(\mathbf{r})$, describes the strength of the coupling between the two internal levels. The total number of BEC atoms, the atomic mass, and the detuning of the em fields from the resonance are denoted by N , m , and δ , respectively.

We assume that the Rabi frequency, $\Omega(\mathbf{r})$, is formed by two appropriately phase-shifted and orthogonal standing em waves, and has the following form:

$$\Omega(\mathbf{r}) = \frac{\Omega_0}{\sqrt{2}}\{\sin[k(x - \bar{x})] - i\sin[k(y - \bar{y})]\}, \quad (3)$$

where k denotes the wave number of the em field. When the phase shifts are equal to zero, $\bar{x} = \bar{y} = 0$, the coupling

vanishes at $x_n = y_n = n\pi/k$, for $n = 0, \pm 1, \pm 2, \dots$. In the close neighborhood of the vanishing Rabi frequency, $|kx_n - n\pi| \ll 1$ and $|ky_m - m\pi| \ll 1$, we obtain

$$\Omega(\mathbf{r}) \simeq (-1)^n \frac{\Omega_0 k \rho}{\sqrt{2}} e^{-\xi i \phi}, \quad (4)$$

with $\xi \equiv (-1)^{n+m}$. Here $\rho \equiv \sqrt{x^2 + y^2}$ is the radial coordinate in the xy plane and ϕ is the corresponding polar angle. In Eq. (1) the phase of the Rabi frequency couples to the relative phase between the two condensates. The phase of $\Omega(\mathbf{r})$ close to a zero-field point in Eq. (4) has the form of the quantized circulation with the unit winding number. We show that the coupling between the em and matter fields establishes a topological relative phase between the two BECs.

To demonstrate the formation of vortices we numerically integrate GPE in two spatial dimensions. For simplicity, we assume that the traps are isotropic ($\alpha_i = 1$), and that the trapping frequencies and the potential minima of the two internal states are equal. As an initial state we assume a nonrotating ground state for a BEC in level $|1\rangle$ and an unoccupied level $|2\rangle$. In the limit of strong self-interaction energy the initial state of ψ_1 may be approximated by the Thomas-Fermi solution in 2D: $\psi_1(\rho) = [2(R^2 - \rho^2)/(\pi R^4)]^{1/2}$, for $R \geq \rho$, and zero otherwise. Here $R \equiv l[4\kappa_{11}^{2D}/(\pi\hbar\omega l^2)]^{1/4}$ denotes the 2D Thomas-Fermi radius of the BEC and $l \equiv [\hbar/(m\omega)]^{1/2}$ is the harmonic trap length scale.

We choose the same ratio between the three scattering lengths, $\kappa_{11}^{2D} : \kappa_{12}^{2D} : \kappa_{22}^{2D} :: 1.03 : 1 : 0.97$, as for ^{87}Rb states $|F=1, m=-1\rangle$ and $|F=2, m=1\rangle$ [23]. In the numerical calculations we use the nonlinearity $\kappa_{12}^{2D}/(\hbar\omega l^2) = 1000$, the Rabi amplitude $\Omega_0 = 50\sqrt{2}\omega$, and the detuning $\delta = 0$. As a first example we create a single vortex with the unit topological charge or the unit quantized circulation. Here the value of the wavelength for the em fields $\lambda = 20l$ and $\bar{x} = \bar{y} = 0$ in Eq. (3), so that only one field node is in the condensate. The atom population is initially in level $|1\rangle$. The em fields start inducing transitions between the two internal levels at time $t = 0$. We decouple the two levels by turning off the em fields at time $t = 0.02/\omega \simeq 1.4/\Omega_0$. In Fig. 1 we display the density $|\psi_2(x, y)|^2$ and the phase ϕ_2 profiles of the BEC atoms in level $|2\rangle$ at $t = 0.0202/\omega$. We observe a vortex in level $|2\rangle$ with a vanishing atom density in the center of the vortex core and the 2π phase winding around the vortex line demonstrating the high quality of the preparation process. The phase profile ϕ_1 of ψ_1 is flat corresponding to a nonrotating state.

The vortex core in Fig. 1 is very large due to the atomic population $|\psi_1(x, y)|^2$ in level $|1\rangle$ which occupies the interior of the vortex and generates a mean-field repulsion as also displayed in Fig. 1. Therefore the presence of the vortex could possibly be directly verified by imaging the density profile of the BEC in level $|2\rangle$ as in Ref. [23]. The relative phase between two BECs has also a dramatic effect on the dynamical structure factor of the two-

component system [24,25] which may be observed, e.g., via the Bragg spectroscopy [26,27].

Next we consider the preparation of several vortices by means of the em fields of Eq. (1). In Fig. 2 we show the density and the phase profiles of rectangular vortex arrays which are obtained with $\lambda = 3l$ (left column) and $\lambda = 5l$ (right column). The plots are evaluated at $t = 0.025/\omega$, when the em fields are still on. The other parameters are the same as in the previous example. The topological phases are distributed according to Eq. (4).

We can investigate the robustness of the prepared vortex states after the turnoff of the em field coupling. The dynamical stability may be studied by integrating GPE with $\Omega = 0$ if we ignore the energetic instabilities due to the interaction of the BECs with thermal atoms [28,29]. In Fig. 3 we show a vortex at a later time with the same set of parameters as in the case of Fig. 1. The em fields are turned off at $t = 0.02/\omega$. At $t = 1.0/\omega$ the phase has acquired a spiral shape indicating a radial inward flow. Although the BECs undergo collective radial oscillations, the vortex remains well preserved several trap periods. In Ref. [23] the radial oscillations were experimentally observed. However, after the initial shrinking period the vortex expanded and broke up. The 2D coherent mean-field picture may not be capable of predicting the breakup. In the case of a vortex array the dynamical deformations are more rapid. However, in our studies we have found that the characteristic features of the vortex pattern with $\lambda = 5l$ (Fig. 2) still exist even at $t = 1.0/\omega$.

With em fields we can generate a variety of different topological structures. If we are able to use transitions through intermediate levels involving several photons, we may prepare several vortices in arbitrary spatial locations with different topological charges. This construction would then exhibit a periodicity determined by the wavelength of the em fields. In a more general case the Rabi frequency from Eq. (3) is determined by

$$\Omega(\mathbf{r}) = \bar{\Omega}_0 \prod_{j=1}^n \{ \sin[\mathbf{k}_j \cdot (\mathbf{r} - \mathbf{r}_0^{(j)})] - i \sin[\mathbf{q}_j \cdot (\mathbf{r} - \mathbf{r}_0^{(j)})] \}^{p_j}. \quad (5)$$

Here we use $|\mathbf{k}_j| = |\mathbf{q}_j|$ and $\mathbf{k}_j \cdot \mathbf{q}_j = 0$. The exponent p_j denotes the topological charge of vortex j and n the number of vortex arrays. For instance, if we use a two-photon transition, we may prepare a vortex with the topological charge of two. In this case we only have the $j = 1$ term with $p_1 = 2$ in Eq. (5).

In Fig. 4 we show a vortex array with the topological charge of two at $t = 0.02/\omega$, when the em fields are still on. In this case $\lambda = 5l$, $\bar{\Omega}_0 = 50\omega$, and the other parameters are the same as before. To reduce the phase noise in the plottings we set the phase in the figures equal to zero when the atom density is very low. Therefore the phase in Fig. 4 is zero close to the vortex line. We note the increase or the decrease in the value of the phase by 4π as individual vortex singularities are encircled.

In Fig. 5 we have prepared a three-fold symmetric pattern of three vortices with the unit topological charge. This is obtained from Eq. (5) with $\mathbf{q}_1/q = \hat{x}$, $\mathbf{q}_2/q = -0.5\hat{x} - 0.87\hat{y}$, $\mathbf{q}_3/q = -0.5\hat{x} + 0.87\hat{y}$, $\mathbf{r}_0^{(j)} = 2.7l\mathbf{q}_j/q$, $\lambda = 2\pi/q = 20l$, and $\Omega_0 = 50\omega$. Butts and Rokhsar [7] have shown that a low-energy state of a rotating BEC can exhibit a similar symmetry. Nevertheless, the low-energy states cannot be directly created even in a rotating trap because the rotation has to overcome the energy barrier to vortex formation [6,7,9].

As a final example we prepare dark solitary waves [17,18] with the Rabi frequency $\Omega(\mathbf{r}) = \Omega_0 \sin(kx)$. In Fig. 6 we display the atom density and phase at time $t = 0.025/\omega$. Here we again use the familiar set of parameters, now with $\lambda = 5l$ and $\Omega_0 = 50\omega$.

In the previous examples we only considered stationary em fields. We may also obtain a time-dependent Rabi frequency by generating a moving standing wave from two nearly counterpropagating em fields with slightly different frequencies. In that case we can move skyrmion vortices inside the BECs along with the moving zero-em-field points in a controlled way.

We proposed a method of generating periodic vortex arrays in a binary BEC. The technique relies on a spatially varying standing em wave configuration which drives atomic transitions between the BECs. A potential experimental limitation is to find em transitions with appropriate wavelengths to produce vortex arrays of different periodicity and number of vortices. Nevertheless, the number of practical transition frequencies may possibly be increased also by tuning the strength of the trapping potential.

In the present work we have demonstrated only in terms of simple examples the formation of vortices and solitary waves. More complicated em field configurations could possibly generate more complex topological structures. The proposed technique could obviously be also generalized to multi-component BECs.

We acknowledge discussions with J. R. Anglin. This work was financially supported by the EC through the TMR Network ERBFMRXCT96-0066.

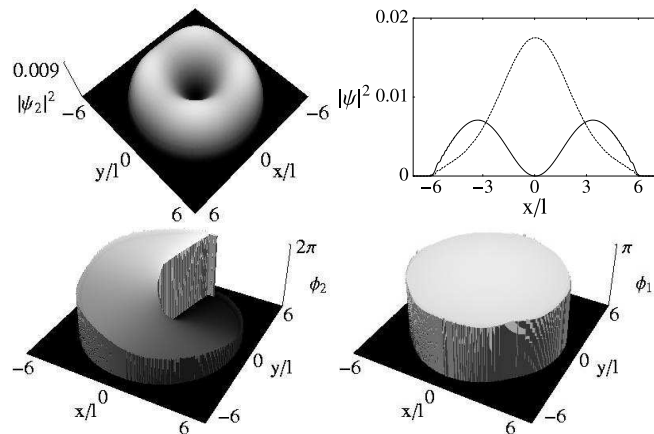


FIG. 1. The preparation of a single vortex with the unit circular quantization. Before the driving em fields are turned on, a nonrotational BEC occupies level $|1\rangle$. The em fields generate a vortex in level $|2\rangle$. We show the density profile $|\psi_2(x,y)|^2$ (upper left) of atoms in level $|2\rangle$, the density along the x axis (upper right) in levels $|2\rangle$ (solid line) and $|1\rangle$ (dashed line), and the phase profiles of levels $|2\rangle$, ϕ_2 , (lower left) and $|1\rangle$, ϕ_1 , (lower right) at a later time. The density and phase of level $|2\rangle$ remarkably clearly display the characteristic properties of a unit-quantized vortex with the 2π phase winding around the vortex core and the vanishing atom density in the center of the core. There is no vorticity in level $|1\rangle$.

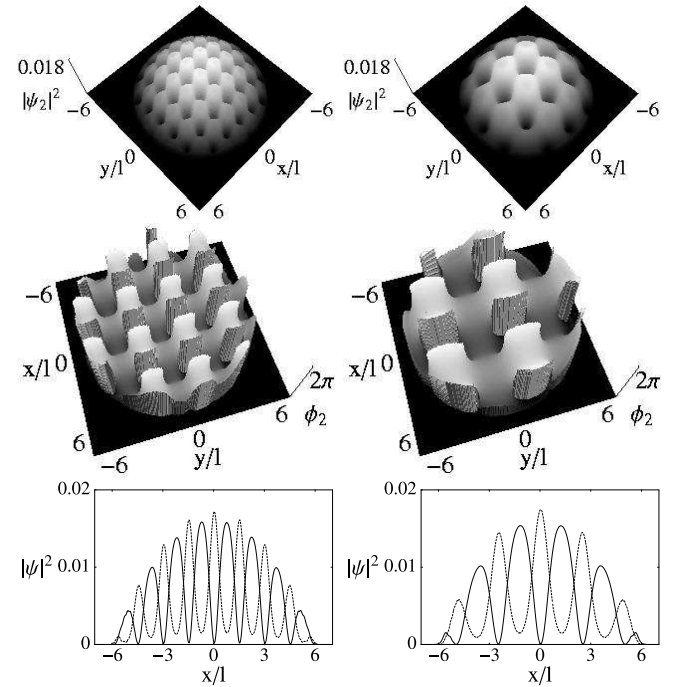


FIG. 2. The preparation of rectangular arrays of vortices with the unit circular quantization. We show the density $|\psi_2(x,y)|^2$ and the phase ϕ_2 profiles of level $|2\rangle$, and the density along the x axis for atoms in levels $|2\rangle$ (solid line) and $|1\rangle$ (dashed line) for $\lambda = 3l$ (left column) and for $\lambda = 5l$ (right column). The circulation around every individual vortex is associated with a 2π change of phase. The flow around the neighboring singularities exhibits opposite helicity.

FIG. 3. The dynamics of a single vortex. We show the phase ϕ_2 of atoms in level $|2\rangle$ at $t = 1.0/\omega$ with the same parameters as in Fig. 1. The spiral shape of the phase indicates inward flow due to radial oscillations. The atom density is displayed in levels $|2\rangle$ (solid line) and $|1\rangle$ (dashed line) at $t = 1.4/\omega$, when the BEC in $|2\rangle$ starts expanding, and in levels $|2\rangle$ (dashed-dotted line) and $|1\rangle$ (dotted line) at $t = 2.5/\omega$.

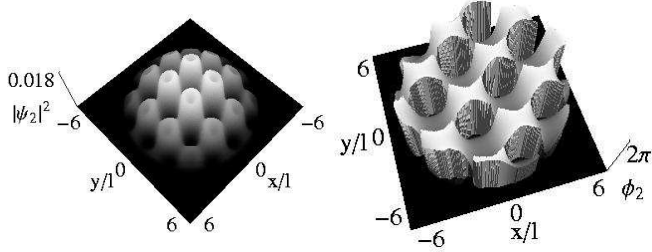


FIG. 4. The preparation of a rectangular array of vortices with the topological charge of two. We show the density and the phase profiles of level $|2\rangle$ for $\lambda = 5l$. The phase profile displays the 4π phase windings around the individual vortex lines.

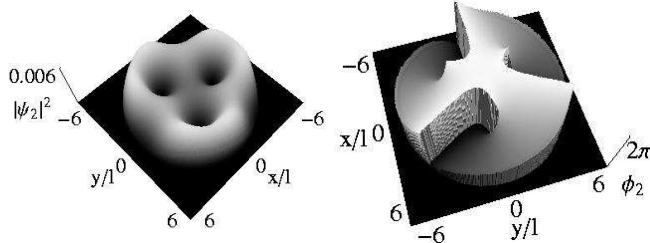


FIG. 5. The preparation of a three-fold symmetric pattern of vortices with the unit circular quantization. We display the density and the phase of atoms in level $|2\rangle$. The circulation around the whole pattern changes the phase by 6π .

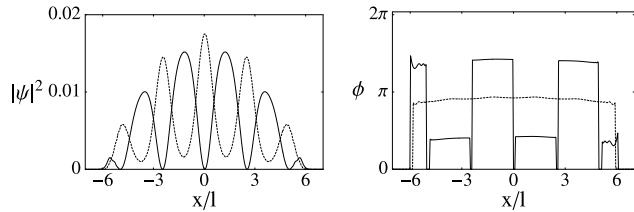


FIG. 6. The preparation of an array of dark solitary waves. We show the density and the phase in levels $|2\rangle$ (solid line) and $|1\rangle$ (dashed line) along the x axis for $\lambda = 5l$. The phase graph displays a sharp phase slip of the order of π in the center of the solitary wave corresponding to the vanishing atom density.

- [1] M. H. Anderson, J. R. Ensher, M. R. Matthews, C. E. Wieman, and E. A. Cornell, *Science* **269**, 198 (1995).
- [2] C. C. Bradley, C. A. Sackett, J. J. Tollett, and R. G. Hulet, *Phys. Rev. Lett.* **75**, 1687 (1995).
- [3] K. B. Davis, M.-O. Mewes, M. R. Andrews, N. J. van Druten, D. S. Durfee, D. M. Kurn, and W. Ketterle, *Phys. Rev. Lett.* **75**, 3969 (1995).
- [4] E.M. Lifshitz and L.P. Pitaevskii, *Statistical Physics, Part II* (Pergamon, Oxford, 1980).
- [5] F. Dalfovo and S. Stringari, *Phys. Rev. A* **53**, 2477 (1996).
- [6] A.L. Fetter, *J. Low Temp. Phys.* **113**, 189 (1998).
- [7] D.A. Butts and D.S. Rokhsar, *Nature* **397**, 327 (1999).
- [8] S. Stringari, *Phys. Rev. Lett.* **82**, 4371 (1999).
- [9] D.L. Feder, C.W. Clark, and B.I. Schneider, *Phys. Rev. Lett.* **82**, 4956 (1999); e-print cond-mat/9910288.
- [10] B. Jackson, J.F. McCann, and C.S. Adams, *Phys. Rev. Lett.* **80**, 3903 (1998).
- [11] B.M. Caradoc-Davies, R.J. Ballagh, and K. Burnett, *Phys. Rev. Lett.* **83**, 895 (1999).
- [12] The evidence for a critical velocity was observed by moving a laser beam through a BEC by C. Raman, M. Köhl, R. Onofrio, D.S. Durfee, C.E. Kuklewicz, Z. Hadzibabic, and W. Ketterle, *Phys. Rev. Lett.* **83**, 2502 (1999).
- [13] K.-P. Marzlin and W. Zhang, *Phys. Rev. A* **57**, 4761 (1998).
- [14] J.R. Anglin and W.H. Zurek, *Phys. Rev. Lett.* **83**, 1707 (1999).
- [15] J. Ruostekoski, B. Kneer, and W.P. Schleich, e-print cond-mat/9908095.
- [16] L. Dobrek, M. Gajda, M. Lewenstein, K. Sengstock, G. Birkl, and W. Ertmer, *Phys. Rev. A* **60**, R3381 (1999).
- [17] K. Helmerson *et al.*, unpublished.
- [18] S. Burger, K. Bongs, S. Dettmer, W. Ertmer, K. Sengstock, A. Sanpera, G.V. Shlyapnikov, and M. Lewenstein, e-print cond-mat/9910487.
- [19] E.L. Bolda and D.F. Walls, *Phys. Lett. A* **246**, 32 (1998).
- [20] K.-P. Marzlin, W. Zhang, and E.M. Wright, *Phys. Rev. Lett.* **79**, 4728 (1997).
- [21] R. Dum, J.I. Cirac, M. Lewenstein, and P. Zoller, *Phys. Rev. Lett.* **80**, 2972 (1998).
- [22] J.E. Williams and M.J. Holland, *Nature* **401**, 568 (1999).
- [23] M.R. Matthews, B.P. Anderson, P.C. Haljan, D.S. Hall, C.E. Wieman, and E.A. Cornell, *Phys. Rev. Lett.* **83**, 2498 (1999).
- [24] J. Ruostekoski and D.F. Walls, *Phys. Rev. A* **55**, 3625 (1997).
- [25] L. Pitaevskii and S. Stringari, e-print cond-mat/9905409.
- [26] D.M. Stamper-Kurn, A.P. Chikkatur, A. Görlitz, S. Innonoue, S. Gupta, D.E. Pritchard, and W. Ketterle, *Phys. Rev. Lett.* **83**, 2876 (1999).
- [27] The phase slip in interference signals vorticity; E.L. Bolda and D.F. Walls, *Phys. Rev. Lett.* **81**, 5477 (1998).
- [28] T. Isoshima and K. Machida, *Phys. Rev. A* **59**, 2203 (1999).
- [29] H. Pu, C.K. Law, J.H. Eberly, and N.P. Bigelow, *Phys. Rev. A* **59**, 1533 (1999).